ChemComm

COMMUNICATION

View Article Online
View Journal | View Issue

Cite this: *Chem. Commun.*, 2017, 53, 4262

Received 13th February 2017,
Accepted 23rd March 2017

DOI: 10.1039/c7cc01138e

rsc.li/chemcomm

Magnetic zeolites: novel nanoreactors through radiofrequency heating†

Jaime García-Aguilar,‡[a] Javier Fernández-García,‡[b] Evgeny V. Rebrov,[bc] Martin Richard Lees,[b] Pengzhao Gao,[d] Diego Cazorla-Amorós[a] and Ángel Berenguer-Murcia *[a]

Many catalytic applications use conventional heating to increase the temperature to allow the desired reaction. A novel methodology is presented for the preparation of magnetic zeolite-based catalysts, allowing more efficient radiofrequency heating. These nanoreactors are tested in the isomerisation of citronellal with successful results and without any apparent deactivation.

Beyond the traditional interest in colloidal particles with controlled structure and/or functionality for the development of catalyst carriers,[1] the synthesis of magnetic nanoparticles has aroused great attention as novel hybrid materials due to the fact that they combine these characteristics with their responsiveness under a high frequency magnetic field which brings forth other interesting features such as the ease of separation or the possibility of heating the said particles using a radiofrequency (RF) coil.[2–3] In this respect, the development of functionalization treatments of high quality to yield materials with superior properties still remains a largely unexplored field, even when significant progress has been reported in the use of different organic and inorganic passivation or functionalization agents.[4,5]

With their exceptional properties in the fields of adsorption and catalysis[6] zeolites are outstanding candidates for the development of advanced composites[7] with magnetic nanoparticles, being one of the possibilities with very promising prospects. The recent works of Zhao *et al.*[1] and Al-Deyab *et al.*[8] have laid the groundwork for two different approaches to the preparation of zeolite-coated magnetic nanoparticles. The first involves coating the as-synthesized magnetic nanoparticles, while the second is achieved *via* the impregnation of zeolite particles with iron salts in order to give rise to magnetic nanoparticles after heat treatment of the resulting composites. Following up on this work, several authors have reported the use of these magnetic zeolites in the removal of different contaminants such as ammonium or heavy metal ions in the liquid phase.[9,10] In these examples, however, the zeolite does not play an active role, merely being an adsorbent for different species, with the added benefit of handling and separation efficiency. The only case which may be found in the literature in which the oxide layer surrounding a magnetic nanoparticle is effectively used as a reaction system is in the very recent work of Cheng *et al.*[11] in which they synthesize TS-1 layers around different magnetic FeO_x species for the photocatalytic degradation of organic contaminants. It should be noted that, even in this example, the reactions are carried out at room temperature, without fully benefitting from any possible synergistic effects between the particle shell and core beyond the well-established ease of separation arising from their magnetic response. Previous reports on the synthesis and application of core@shell particles have endeavoured to combine the properties of both parts of the material so that they may act in a combined and effective manner. Okada *et al.*[12] and Mori *et al.*[13] presented a core–shell structured catalyst (Pd and FeO_x core, respectively) into a SiO_2 matrix in one-pot oxidation reactions. Another similar example was reported by Ceylan *et al.*[14] where Fe_3O_4/Fe_2O_3 particles coated by Pd-loaded silica were applied in different coupling reactions by RF heating. Nishiyama *et al.*[15] synthesized zeolite-encapsulated Pt/TiO_2 catalysts for the hydrogenation of different C6 hydrocarbon mixtures, with the zeolite layer acting as a permselective barrier and the particle core playing an active role in hydrogenating the permeating reagents. In this respect, it would be interesting if the core of a magnetic zeolite could contribute to the performance of the prepared material in a manner different (yet complementary) to what has been reported to date.

In this work we aim to prepare zeolite shells encapsulating magnetic nanoparticles by subjecting a suspension of TiO_2-coated

[a] *Inorganic Chemistry Department and Materials Science Institute, Alicante University, Ap. 99, E-03080 Alicante, Spain. E-mail: a.berenguer@ua.es*
[b] *University of Warwick, Coventry, CV4 7AL, UK*
[c] *Department of Biotechnology and Chemistry, Tver State Technical University, Tver 170026, Russia*
[d] *College of Materials Science and Engineering, Hunan University, Changsha, 410082, China*

† Electronic supplementary information (ESI) available. See DOI: 10.1039/c7cc01138e

‡ These authors contributed equally to the manuscript.

nickel ferrite nanoparticles to hydrothermal treatment (static or dynamic) in an aqueous ZSM-5 precursor solution. The resulting composites show a ferrite core with a well-defined shell of zeolite ZSM-5 with a mean particle size ranging between 0.5 and 2 microns, and show a coercive field of $\approx$0.0085 T and a permanent magnetization of $\approx$0.2 A m^2 kg^{-1} (which would correspond to 0.34 wt% of magnetic material in the composite materials, see Fig. S1, ESI†), and exhibit good dispersability in water. The resulting solids are then applied in the isomerisation reaction of citronellal to isopulegol with promising results. This paper thus constitutes a landmark in the combination of RF heating in ferrite@zeolite particles for the development of nano-reactors with an unparalleled level of reaction control.

In a typical synthesis (see the ESI† for full experimental details), the nickel ferrite nanoparticles were synthesized following a protocol adapted from the literature.[16] A portion of the magnetic nanoparticles with a magnetic domain size between 40 and 50 nm (calculated from their coercivity) was sonicated using an aqueous solution of tetrapropylammonium hydroxide (TPA-OH) which acts as a templating agent for the zeolite and as a surfactant which adsorbs on the surface of the nanoparticles, facilitating their dispersion (the ferrite particles sedimented in a few seconds after sonication in the absence of TPA-OH). The obtained dispersion was used in the hydrothermal synthesis of a zeolite in order to encapsulate each magnetic nanoparticle in a zeolite shell as described in the ESI.† Two different growth regimes in a Teflon autoclave were employed: static or dynamic synthesis. In both cases, however, while no uncoated magnetic particles were observed (see Fig. S2, ESI†), there was a significant fraction of zeolite crystals which were formed in solution rather than encapsulating the nickel ferrite particles. This fact is revealed in Fig. 1, which shows the Scanning Electron Microscopy (SEM) and Transmission Electron Microscopy (TEM) images of a sample obtained in the dynamic synthesis, where particles with distinct surface morphologies are observed; the particles with a characteristic coffin shape and smooth surface are ZSM-5 crystals which had grown in solution whereas the particles in which the planes grown along the *a* and *c* directions are significantly different from typical MFI zeolites (which we may call a ''rough grain'' surface) were the magnetic ferrite nanoparticles encapsulated in very small zeolite crystals. The core@shell structure of the synthesized materials can be further confirmed by comparing the obtained FE-SEM/TEM images with those of the pure nickel ferrite (Fig. S2, ESI†).

It must be noted that the same micrographs taken from the samples obtained under static conditions showed a similar type of nanoparticles, although the fraction of particles with a rough grain surface was smaller than that obtained under dynamic conditions (Fig. S3, ESI†), confirming that conditions favouring homogeneous crystallization were more conductive towards the successful coating of ferrite nanoparticles. X-Ray diffraction analysis (Fig. S4, ESI†) confirmed the presence of both MFI and ferrite phases in all samples. Nitrogen physisorption analyses (Table S1, ESI†) revealed that samples prepared by both methods had similar porosities, with the samples obtained under dynamic conditions showing a slightly higher value (350 and 310 m^2 g^{-1} for the dynamic and static samples, respectively). This difference may be attributed to increased adsorption on the surface roughness in the sample prepared under dynamic conditions. The pore volume values obtained for both samples were practically identical (0.15 and 0.14 cm^3 g^{-1} for the two samples), which are slightly lower, due to the presence of the non-porous nickel ferrite in the composite, than previously reported values for this type of zeolites.[17]

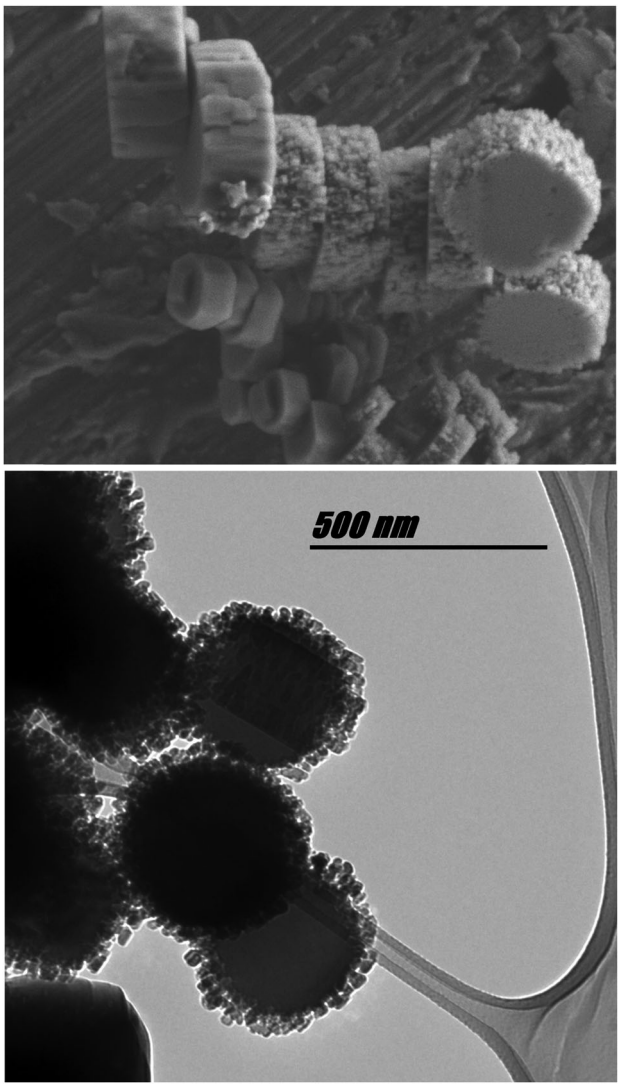

Fig. 1 FE-SEM (top) and TEM (bottom) micrographs of the zeolite-encapsulated magnetic nanoparticles obtained under dynamic conditions.

It must be noted that the TiO_2 shell deposited around the nickel ferrite nanoparticles was critical for the successful preparation of the core@shell structure reported in this study. When bare nickel ferrite nanoparticles were added to the autoclaves and subjected to hydrothermal treatment the filtered solid particles did not contain any ferrite particles (evidenced both by their colour and the corresponding TEM images). Thus, the TiO_2 shell plays a key role in the successful preparation of core@shell structures, acting as a linker under the employed conditions, as we have reported for similar systems.[18]

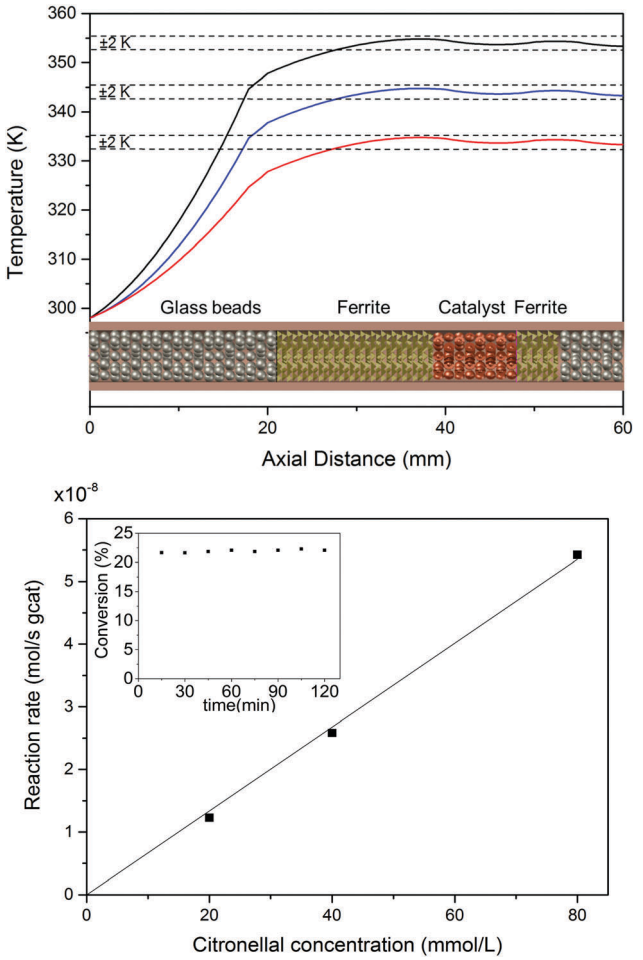

Fig. 2 Temperature profiles in the reactor at three set-points of 333, 343 and 353 K (top). Reaction rate as a function of the initial concentration of citronellal. Temperature 353 K (inset: conversion as a function of time on stream) (bottom). Catalyst weight: 82.2 mg. Liquid flow rate: 0.1 ml min^{-1}. Gas flow rate: 3.0 ml min^{-1} (Standard Temperature and Pressure (STP)).

Benefitting from the fact that the core of the composite nanoparticles is sensitive to a magnetic field (the magnetic heating generation rate was determined for both sets of samples presenting a value of ≈ 0.2 W g^{-1}), the reactor configuration was chosen so as to achieve efficient isothermal heating (see the ESI†).[19] As shown in Fig. 2 (top), the packed bed configuration not only allows one to reach the desired reaction temperature within seconds of applying the RF field, but also allows the reaction temperature to be controlled within a very narrow range (around 2 K). Additionally, this configuration also avoids the formation of non-uniform temperature distributions and hot spots[20] and overcomes the drawbacks in the scale-up of microreactors.[21]

Such a configuration has an inherently large surface area-to-volume ratio, offering high heat and mass transfer rates, which is beneficial for attaining high conversion rates and enables optimum control of the residence time and temperature distribution. Moreover, the results for this configuration with nickel ferrite were satisfactory in previous works[19,22] but now the magnetic contribution from the magnetic zeolite to RF heating makes the profile more stable. The results obtained show that citronellal isomerisation has been successfully achieved with RF heating.

RF heating with magnetic materials has previously been used for other reactions[19,22] and has been shown to be a suitable way to produce heating, even on an industrial scale.[21] These new magnetic materials widen the possibilities of using RF heating as a more efficient, green alternative to conventional heating that can be applied on an industrial scale. Most importantly, heating is restricted to the core–shell particles (specifically to their core), and thus this type of reactor is both novel in its conception and of almost unrivalled efficiency.

Considering the data obtained for the isomerisation of citronellal presented in Fig. 2 (bottom) (main panel), a linear dependence of the reaction rate with the reactant concentration suggests a first-order dependence with respect to citronellal. Moreover the light-off curves overlapped for the different initial concentrations, also indicating a linear dependence. As the temperature increases from 323 to 353 K, the citronellal conversion increases from 6 to 22% (see the light-off curves for this reaction in Fig. S5, ESI†). The isomerisation of citronellal was performed over the magnetic zeolite (specifically ZSM-5) which provides a high isomerisation rate due to its high Brønsted acidity.[23] The apparent activation energy of 44.9 kJ mol^{-1} was obtained from the temperature dependence of the reaction rates. A comparable value of 55 kJ mol^{-1} was reported by Yongzhong *et al.*[24] over a Zr/Beta zeolite catalyst. No further studies were performed above the 353 K limit as a rapid catalyst deactivation was observed above 353 K in line with the data reported by Mäki-Arvela *et al.*[23]

The catalyst is stable as no deactivation is observed for a period of 120 min. The catalyst seems to be stable reaching a constant conversion of 22%. The mass of the catalyst was measured before and after the reaction showing a difference of around 0.5% and the morphology of the particles remained unchanged after testing, which indicates the excellent mechanical stability of the magnetic catalyst. Moreover, this new magnetic zeolite allows simple separation of the catalyst using an external magnet,[25] which as already mentioned gives added value of the active phase in terms of handling and reuse. This kind of reaction has become one of the most active research areas in pharmaceutical and fine chemical industries.[14,26–29]

For comparison purposes, the same microreactor experiments were performed with a physical mixture of ferrite and the zeolite. The first attempts to prepare physical mixtures with compositions as similar as possible to our core@shell composite (2/98 wt%) resulted in highly heterogeneous mixtures which performed very poorly in the isomerization of citronellal. Thus, we increased the amount of nickel ferrite until a homogeneous mixture was obtained, which was 50/50 wt%. In Table S2 (ESI†), it can be seen that the normalized reaction rate for the physical mixture is quite similar to the one obtained for the magnetic composite. Therefore, this means that the properties of the zeolite remain unchanged by varying the quantity of ferrite present in the reaction mixture. The surface area and pore

volume for this zeolite in the physical mixture were analyzed before and after the reaction, with negligible changes in both the surface area and the pore volume of the mechanical mixture, with values very similar to those mentioned above. All these measurements indicate that the physical mixture can be assumed to be similar to the magnetic composite and its properties are not affected after the reaction, so the catalyst is stable.

In summary, TiO_2–$NiFe_2O_4$@zeolite (ZSM-5) particles have been synthesized by a simple two-step process in which TiO_2-coated nickel ferrite particles are coated with a layer of ZSM-5 zeolite crystals after dispersion in the presence of a surfactant (which is the zeolite structure directing agent). Performing the hydrothermal synthesis of the zeolite layer using dynamic conditions allows for a larger fraction of coated ferrite particles over the static synthesis, which ultimately results in a higher yield towards the desired product. The resulting core@shell structures have been incorporated into a structured reactor configuration in which citronellal is isomerized to isopulegol with exceptional control of the conditions inside the reactor, allowing for the development of reactors and reaction systems with outstanding performance and stability, surpassing by a 25-fold factor the behaviour of a similar physical ferrite/zeolite mixture.

We thank the MINECO, GV, and FEDER (Projects CTQ2015-66080-R MINECO/FEDER, BES-2013-063678 and PROMETEOII/2014/010) for financial support. Moreover, the financial support provided by the European Research Council (ERC), project 279867, and Russian Science Foundation (project 15-13-20015) is gratefully acknowledged.

Notes and references

1 Y. Deng, C. Deng, D. Qi, C. Liu, J. Liu, X. Zhang and D. Zhao, *Adv. Mater.*, 2009, **21**, 1377.
2 P. Gao, E. V. Rebrov, M. W. G. M. Verhoeven, J. C. Schouten, R. Kleismit, G. Kozlowski, J. Cetnar, Z. Turgut and G. Subramanyam, *J. Appl. Phys.*, 2010, **107**, 044317.
3 A. Zadrazil, V. Tokarova and F. Stepanek, *Soft Matter*, 2012, **8**, 1811.
4 W. Wu, Q. He and C. Jiang, *Nanoscale Res. Lett.*, 2008, **3**, 397.
5 A. Bordet, L.-M. Lacroix, P.-F. Fazzini, J. Carrey, K. Soulantica and B. Chaudret, *Angew. Chem., Int. Ed.*, 2016, **55**, 15894.
6 E. G. Derouane, *J. Mol. Catal. A: Chem.*, 1998, **134**, 29.
7 A. Berenguer-Murcia, J. García-Martínez, D. Cazorla-Amorós, A. Linares-Solano and A. B. Fuertes, *Microporous Mesoporous Mater.*, 2003, **59**, 147.
8 T. A. Salah El-Din, A. A. Elzatahry, D. M. Aldhayan, A. M. Al-Enizi and S. S. Al-Deyab, *Int. J. Electrochem. Sci.*, 2011, **6**, 6177.
9 M. Liu, B.-D. Xi, L.-A. Hou and S. Yu, *J. Mater. Chem. A*, 2013, **1**, 12617.
10 H. Liu, S. Peng, L. Shu, T. Chen, T. Bao and R. L. Frost, *Chemosphere*, 2013, **91**, 1539.
11 Q. Lv, G. Li, H. Lu, W. Cai, H. Huang and C. Cheng, *Microporous Mesoporous Mater.*, 2015, **203**, 202.
12 S. Okada, K. Mori, T. Kamegawa, M. Che and H. Yamashita, *Chem. – Eur. J.*, 2011, **17**, 9047.
13 K. Mori, Y. Kondo, S. Morimoto and H. Yamashita, *J. Phys. Chem. C*, 2008, **112**, 397.
14 S. Ceylan, C. Friese, C. Lammel, K. Mazac and A. Kirschning, *Angew. Chem., Int. Ed.*, 2008, **47**, 8950.
15 N. Nishiyama, K. Ichioka, M. Miyamoto, Y. Egashira, K. Ueyama, L. Gora, W. Zhu, F. Kapteijn and J. A. Moulijn, *Microporous Mesoporous Mater.*, 2005, **83**, 244.
16 P. Gao, X. Hua, V. Degirmenci, D. Rooney, M. Khraisheh, R. Pollard, R. M. Bowman and E. V. Rebrov, *J. Magn. Magn. Mater.*, 2013, **348**, 44.
17 S. Sartipi, K. Parashar, M. J. Valero-Romero, V. P. Santos, B. van der Linden, M. Makkee, F. Kapteijn and J. Cascon, *J. Catal.*, 2013, **305**, 179.
18 J. García-Aguilar, I. Miguel-García, Á. Berenguer-Murcia and D. Cazorla-Amorós, *ACS Appl. Mater. Interfaces*, 2014, **6**, 22506.
19 S. Chatterjee, V. Degirmenci, F. Aiouache and E. V. Rebrov, *Chem. Eng. J.*, 2014, **243**, 225.
20 J. G. Boelhouwer, H. W. Piepers and A. A. H. Drinkenburg, *Chem. Eng. Sci.*, 2001, **56**, 1181.
21 J. Fernandez, S. Chatterjee, V. Degirmenci and E. V. Rebrov, *Green Process. Synth.*, 2015, **4**, 343.
22 S. Chatterjee, V. Degirmenci and E. V. Rebrov, *Chem. Eng. J.*, 2015, **281**, 884.
23 P. Mäki-Arvela, N. Kumar, V. Nieminen, R. Sjoholm, T. Salmi and D. Y. Murzin, *J. Catal.*, 2004, **225**, 155.
24 Z. Yongzhong, N. Yuntong, S. Jaenicke and G. K. Chuah, *J. Catal.*, 2005, **229**, 445.
25 T. K. Houlding and E. V. Rebrov, *Green Process. Synth.*, 2012, **1**, 19.
26 M. J. Climent, A. Corma, S. Iborra and M. J. Sabater, *ACS Catal.*, 2014, **4**, 870.
27 D. E. Fogg and E. N. dos Santos, *Coord. Chem. Rev.*, 2004, **248**, 2365.
28 X. Zeng, *Chem. Rev.*, 2013, **113**, 6864.
29 D. M. Roberge, L. Ducry, N. Bieler, P. Cretton and B. Zimmermann, *Chem. Eng. Technol.*, 2005, **28**, 318.